10-2021

Effects of Air-Injection Pressure on Airflow Pattern of Air Sparging

Arvin Farid
Boise State University

Atena Najafi
Boise State University

Jim Browning
Boise State University

Elisa Barney Smith
Boise State University

Airflow Pattern During Air Sparging. I: Air Pressure Effect

Arvin Farid, Ph.D., P.E., M.ASCE*
Associate Professor
Department of Civil Engineering
Boise State University
Boise, Idaho, USA
ArvinFarid@BoiseState.edu

Atena Najafi
Graduate Research Assistant
Department of Civil Engineering
Boise State University
Boise, Idaho, USA

Jim Browning, Ph.D.
Associate Professor
Department of Electrical & Computer Engineering
Boise State University
Boise, Idaho, USA

Elisa Barney Smith, Ph.D.
Professor
Department of Electrical & Computer Engineering
Boise State University
Boise, Idaho, USA

Abstract

Air sparging is a popular remediation technology for treating soil and groundwater contaminated with volatile organic compounds (VOCs). The VOC removal process during air sparging is rendered ineffective because of the random formation of air channels, creating preferential paths for airflow and, in turn, limiting remediation to these channels referred to as zone of influence (ZOI). Pulsation is a popular method used to improve the effectiveness of air sparging through cyclic operation, which is more time-consuming. This paper presents a laboratory investigation of the effects of initial and further increases in the injected air's pressure on airflow pattern within a glass-bead medium used as an analogous medium to soil. Digital images of the airflow patterns were collected; these images show an increase in the radius of influence (ROI) and ZOI due to the initial air-pressure increase, especially when a higher overburden pressure (dry soil simulant) is available above the water-saturated zone. Further increases in the air pressure seem to have no measurable effect on the ROI and the shape of the ZOI.

Keywords: remediation, air sparging, airflow, zone of influence, radius of influence, pressure

Introduction

Groundwater contamination has become a widespread problem in need of urgent attention from various federal and state agencies. Thus, remediation of contaminated soil and groundwater is of interest to these agencies. Several remediation techniques have been used to remove contaminants, among which air sparging is very popular (Johnson et al., 1998; Michael and Ken, 2006). Air sparging is an in-situ technique used for remediation of groundwater and saturated soils contaminated with volatile organic compounds (VOCs). Air sparging came into existence about 1985 in Germany and is becoming increasingly popular in the United States.

Soil vapor extraction (SVE) is another common treatment technology used alone or more often in conjunction with air sparging to remediate soil above the water table (i.e., within the vadose zone) where volatile contaminants are removed from the soil by vacuum pumps. SVE is effective for the remediation of the vadose zone but cannot be employed in the saturated zone. It is usually used in combination with air sparging to extract VOCs already volatilized by air sparging and moved into the vadose zone. Fig. 1 shows a schematic image of an air-sparging system.

During air sparging, pressurized air is injected into saturated water. The injected air then flows up to the surface, creating air passageways. The contaminants within these air passages are thus volatilized. The vapors are then captured through soil-vapor-extraction wells. Air sparging can also be used to mitigate liquefaction (Marley et al., 1996). During an earthquake, due to the sudden rise in the excess pore-water pressure (in excess of hydrostatic pressure), a sudden drop in the effective stress can occur, resulting in the loss of shear strength in saturated, loose sandy layers. This process is called liquefaction, which is the source of large settlements and foundation/structure damage (Yegian et al., 2007). Research

has shown that a small reduction in the degree of saturation of fully water-saturated sands can result in mitigation of the shear-strength loss due to liquefaction. Yegian et al. (2007) proposed and proved that a method referred to by them as IPS (induced partial saturation) can also mitigate liquefaction.

Air sparging used for remediation or liquefaction mitigation is, however, limited by random air-channel formation (Elder and Benson, 1999; Farid et al., 2015; Azad et al., 2013), which creates a mass transfer zone (MTZ) of limited size within and adjacent to formed air channels (Braida and Ong, 2001; Ji et al., 1993). Therefore, the current air-sparging practice can take months or years, can be costly and ineffective, and can lead to incomplete remediation. One of the most popular methods to enhance air sparging's effectiveness is pulsating the air-injection pumps (Benner et al., 2002), hoping new air channels will be created elsewhere. Pulsation is also time-consuming and not guaranteed to create new air channels elsewhere. In other words, the initial channels may displace soil particles, creating preferential paths for new channels, which prevents new air channels from being formed elsewhere, thus, preventing the MTZ from spreading into untreated regions. Hu et al. (2010) studied the effect of soil-grain size and initial-injection air pressure on the ZOI angle with the vertical line and the vertical profile of the ZOI shape.

This study focuses on the major goal of understanding the effect of the initial and any further increase in the injected air's pressures and overburden pressure (due to the unsaturated soil layer) on air-channel formation (especially the ROI) within saturated soil, in order to find ways to enhance air sparging's effectiveness.

Background

Soil Characteristic Phase Parameters

Soil porosity (n) and void ratio (e) refer to the part of a soil volume not occupied with soil particles or organic matter. Pore spaces are usually filled with air, other gases, or water. Porosity and void ratio are measures of void spaces in soil (V_v). Porosity is the ratio of the void volume over the total volume (V_t) usually presented in percentage (0% – 100%).

$$n = \frac{V_v}{V_t} \times 100\% \tag{1}$$

Void ratio (e) is the ratio of the void (V_v) volume over the volume of solids (V_s).

$$e = \frac{V_v}{V_s} \tag{2}$$

The degree of saturation (S) is the ratio of the liquid (such as water) volume (V_w) to the void volume in a porous material such as soil (V_v), usually presented in percentage.

$$S = \frac{V_w}{V_v} \times 100\% \tag{3}$$

Major Design Factors for Air Sparging

A working knowledge of the extent and nature of airflow through saturated soils is important in order to find the optimum design of air-sparging systems and the estimation of this field performance. The zone of influence (ZOI) is defined as the region of soil treated by a given injection or extraction well. The radial distance from the well to the outer edge of this zone is known as the radius of influence (ROI). The ROI is a critical design parameter for a field system because an overestimated ROI will lead to inadequate subsurface treatment while an underestimated ROI will lead to an unnecessary number of wells. The efficiency of an in-situ air-sparging system is controlled by the extent of contact between the injected air and contaminated soil as well as the residence time of air in soil. The zone of influence (ZOI), the airflow pattern, and air distribution during remediation using air sparging are major design factors (Semer, 1998). Lundegrad and Andersen (1996) reported that the ZOI was cone-shaped, while several other researchers reported parabolic-shaped ZOI. They all agree that the size of the ZOI becomes smaller for soils with larger-sized particles. The angle of ZOI, which is the angle between the vertical axis and the ZOI boundary, has been reported to be between 15° for gravel and 56° for fine sands (Nyer and Suthersan, 1993; Suthersan and Raton, 1999, Reddy and Adams, 2001; Reddy el., 1995).

Gas-Phase Flow Pattern

According to research by Semer et al. (1998), two types of gas-phase flow patterns are formed in in-situ air sparging (ISAS) based on the properties of the soil: (i) air-bubble flow pattern and (ii) air-channel flow pattern. The gas-phase distribution during ISAS is complex due to the intricate nature of aquifer material and the forces controlling the multiphase flow within porous media. Multiple airflow patterns (both bubbles and channels) may exist depending on the aquifer characteristics, especially if a double-porosity nature exists. A fundamental understanding of mechanisms determining the occurrence of each pattern is important in order to better design air sparging. Pore size, which is generally dependent on grain size, plays the primary role in determining the flow pattern (Semer, 1998). Air-channel formation will occur in porous media with grains equal to or less in size than 1 to 2 mm (Brooks et al., 1999); this is in a very uniform gradation case. Air-bubble formation will generally occur in media with grains greater in size than 1 to 2 mm (Brooks et al., 1999).

Methods to Prepare Homogeneous Soil Samples

There are several methods of homogenous soil-sample preparation. The pluviation method is a method to prepare homogenous granular media. There are two types of pluviation methods: wet pluviation and dry pluviation. Dry- and wet-pluviation methods are used to prepare dry or fully water-saturated samples, respectively. In the wet-pluviation method, the water will be poured up to a predetermined level, and then soil will be gently and uniformly poured into the water through a uniformly moving funnel. In the dry-pluviation method, the soil will be uniformly poured into the container through a uniformly moving funnel. These methods offer several advantages, including higher, better-controlled dry density; no particle crushing; less segregation; and better repeatability. In addition, the pluviation method can be performed with greater facility in shorter time in comparison with other methods. We selected the wet-pluviation method to prepare the water-saturated layer, which is a specimen preparation technique very well suited for preparation of large, fully water-saturated, homogeneous specimens of this work (Bayat et al., 2009).

Materials and Methods

The experiments were performed in a 61.5cm × 40cm × 15cm clear acrylic tank. Digital imaging of the top of the tank was performed to quantitatively analyze the airflow induced into fully water-saturated glass-bead media and to determine, in future experiments, the electromagnetic (EM) stimulation effect on air sparging. The EM stimulation effect does not fit within the scope of this paper and is explained in another paper by the authors (Farid et al., 2015). The imaging was performed using a Cannon Rebel T2i 18-Megapixel digital camera.

Fig. 1 shows the test apparatus used for air sparging through the glass-bead medium and the location of the air-injection well. The test-apparatus walls are 0.6 cm thick. Three perforated acrylic panels covered with geotextile fabric were placed at the bottom and the two sides of the tank to create three rechargeable reservoirs. Geotextile was used to create the rechargeable reservoirs. Thus, water can easily pass through the geotextile, but glass beads cannot. The compartment surrounded by the three perforated panels was used to contain the glass-bead medium. The three regions between the perforated inner panels and the solid outer walls act as reservoirs for water, aiding seepage regulation, stabilization of the water table, or drainage/recharge. An inflow valve was installed on the front side of the tank at a height of 3 cm above the bottom reservoir's bottom. Two outflow valves were installed on the outer sides of the side reservoirs at a height of 20 cm above their bottom. Two removable PVC stiffeners were designed and installed to provide more stiffness to the box.

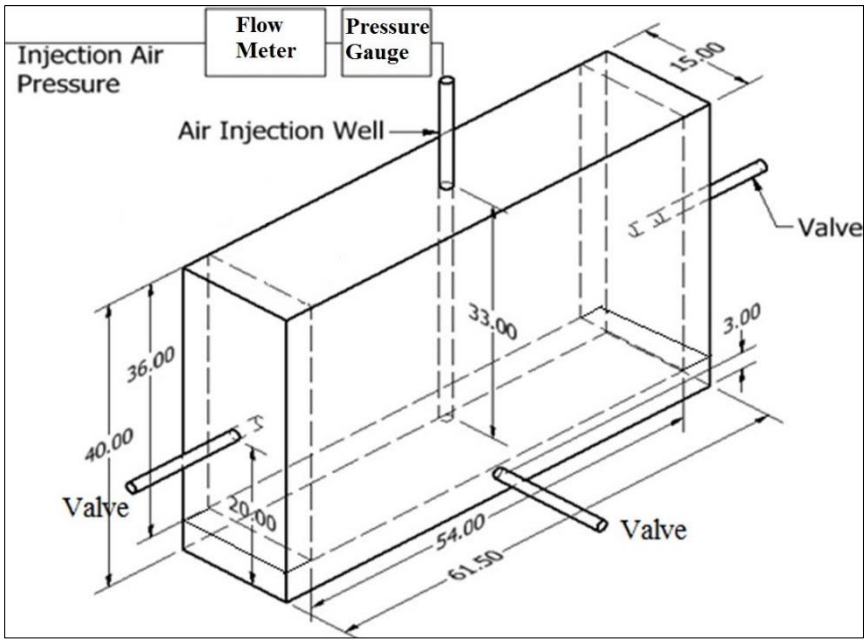

Fig. 1. Schematic of 61.5cm × 40cm × 15cm experimental box.

A PVC tube was used to simulate the air-injection well. The tube has a 2.15cm outside diameter, 1.6cm inside diameter, and 50cm length. Four 1.6mm diameter holes were drilled symmetrically along the lower 3 cm of the tube to allow symmetric air transfer into the glass-bead medium. The end of the tube is plugged. An acrylic plate was placed above the tank to support the tube in its proper location within the box. The tube, used for air injection, was placed in the middle of the top plate with its plugged bottom resting 3 cm above the bottom of the glass-bead-filled middle compartment (7 cm above the tank bottom). The injection tube is connected to an air-supply faucet provided in the lab. Fig. 2 shows the air-injection setup in detail.

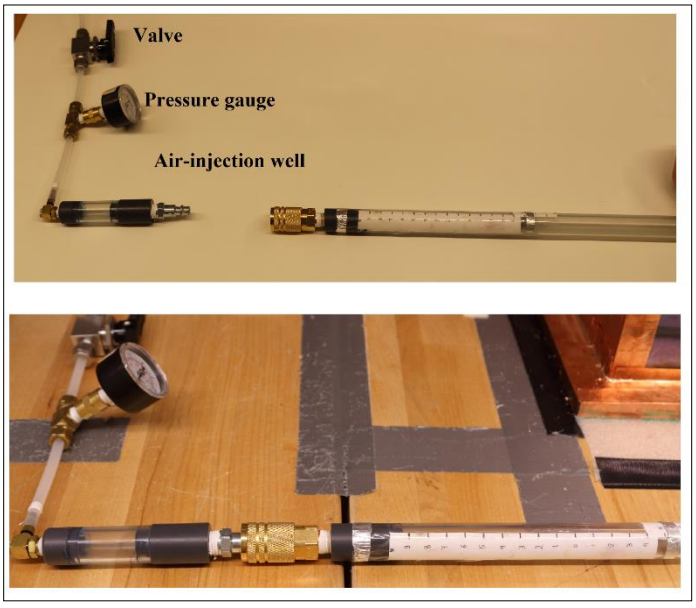

Fig. 2. Adjustable air-injection well, including pressure gauge and valve.

The air-injection system was designed to inject air in a symmetric way. A ¼inch clear PVC tube was used as a connection between the source of air and the air-injection tube. A flowmeter was provided to measure the airflow rate, located before the air-injection well. A pressure gauge was located right after the flowmeter to measure the air-injection pressure entering the well (Fig. 2). A Dwyer VFA-8-BV flowmeter was used for this study, which is proper for the pressure range of this study. The scale unit of this flowmeter is SCFH (standard cubic feet per minute of volumetric flow rate of gas at the set standard condition of 49o C maximum temperature and 960 kPa for pressure, Fig. 3). A camera was located at the top of the box to take top-view images of the ZOI. Another camera was also placed against the front side of the box to take front-view images.

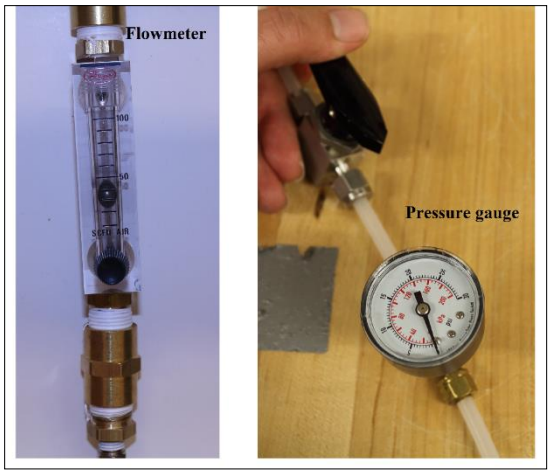

Fig. 3. Flowmeter and pressure gauge.

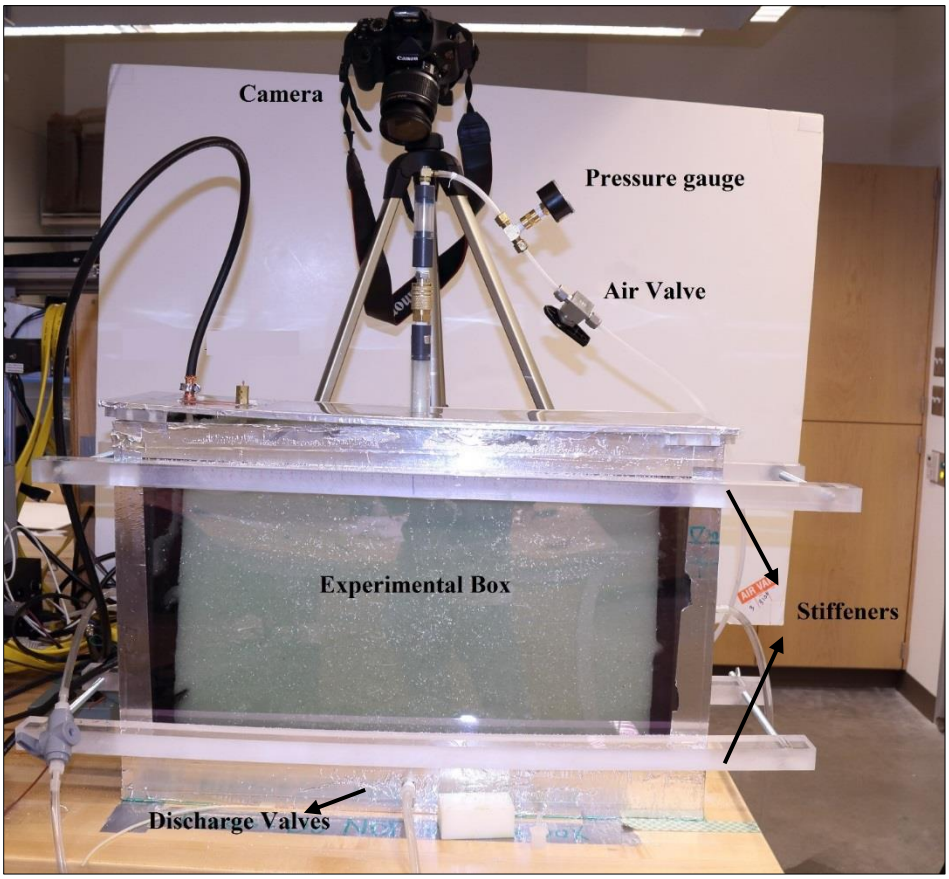

Fig. 4. Experimental box including air-injection well, three recharge valves, loop antenna, stiffeners, and camera.

The opacity of natural soil prevents the direct observation of airflow patterns during air sparging. Hence, transparent glass beads were used in this study to both simulate the natural soil and facilitate visual observation. Glass beads used for this study are Class-A Ballotini impact-beads from Potters Company with a specific gravity of 2.46 g/cm3. Table 1 shows the properties of the glass beads.

Table 1. Properties of Glass Beads.

Potters Designation	U.S. Sieve #	Maximum Size (Inches)	Minimum Size (Inches)	Maximum Size (Microns)	Minimum Size (Microns)	Minimum % of Round Beads
Class A	20-30	0.0331	0.0234	850	600	65

Both wet and dry pluviation were used to prepare the fully water-saturated and dry sample, respectively. As mentioned, during the wet-pluviation method, water was first poured into the box up to a predetermined level. The amount of water was predetermined for each configuration of the tests according to their design. Glass beads were then gently poured into water using a funnel located 20 cm above the water table in order to allow for preparation of a homogenous fully water-saturated glass-bead medium. The top surface of the glass-bead medium was gently smoothed over, and pooling of water on top of the soil was not allowed. This process was performed carefully to avoid the creation of layering to avoid possible creation of preferential air-passage paths. This procedure was continued until the desired thickness of the medium was reached (Table 2). The mass and volume of the placed glass beads were measured, and the porosity of the medium was then calculated.

Experiment Procedure

Two configurations (C1and C2) were designed and prepared, and airflow patterns were observed for those two configurations. These configurations (C1and C2) were designed to evaluate the effect of the thickness of a partially saturated zone and the homogeneity of the configuration of the ZOI during air sparging. These two configurations (C1and C2) have the same thickness of fully water-saturated glass beads but are different in the thickness of the partially saturated zone and air (Fig. 5). Table 2 shows the properties of these configurations, and Fig. 5 shows schematic Configurations C1and C2. In theory, it is desired that both configurations (C1 and C2) be identical and, hence, have the same porosity, but because of the pluviation method and as in any other experimental work, the actual porosities of the two configurations are slightly different (by 2%).

Table 2. Properties of Glass-Bead Configurations

Configuration No.	Particle Size (mm)	U.S. Sieve #	Total Height of Sample (cm)	Height of Saturated Layer (cm)	Height of Unsaturated Layer (cm)	Porosity
C1	0.6-0.85	20-30	28	24	4	62%
C2	0.6-0.85	20-30	36	24	12	60%

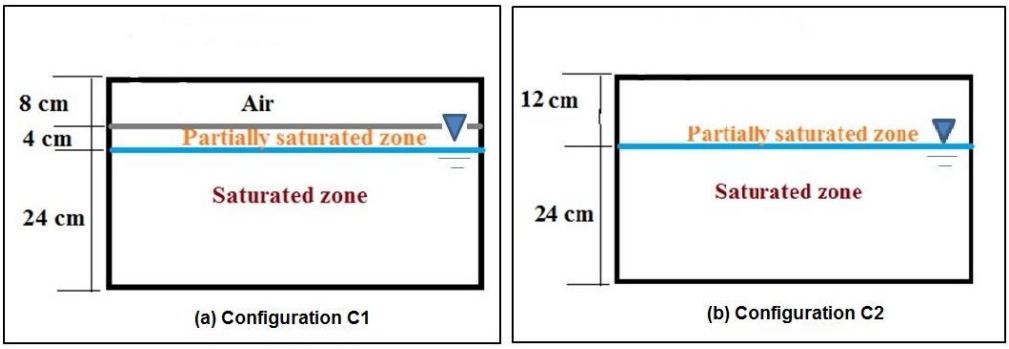

Fig. 5. Schematics of two configurations with various thicknesses of partially saturated zones: a) Configuration C1, b) Configuration C2.

To prepare Configuration C1 using dry and wet pluviation methods, water was first poured to a predetermined level of 18 cm (16.8 liters), and then 24.6 kg of glass beads were gently poured through a funnel located 20 cm above the water table into water using the wet pluviation technique (Vaid and Negussey, 1998). Fig. 6 shows the medium preparation. The process of sample preparation for Configuration C2 is the same as that of Configuration C1, except the thickness of the amount of the dry zone is different. For Configuration C2, 16.8 L of water and 29 kg of glass beads were used.

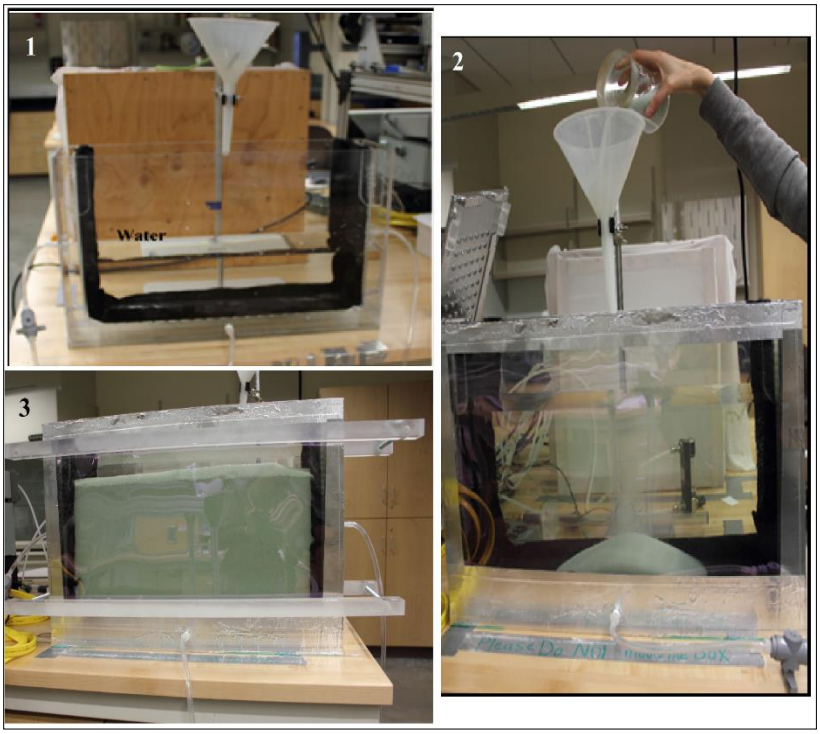

Fig. 6. Preparing Configuration C2 in clean soil lab using wet-pluviation method.

Air injection into the medium was performed at various air-pressure levels from 14 to 60 kPa. The air-injection pressure was measured at the entrance of the injection well. Then, after the channels were formed, the airflow pattern was observed on the front face of the box. The airflow rate was also measured using a flowmeter (Dwyer VFA-8-BV). Table 3 shows the experimental conditions for various air-injection pressure levels. Every experiment presented in this paper was repeated at least three times to confirm the repeatability of experiments. The size of ROI measured in all repetitions (i.e., repeats at the same initiation air pressure) did not change, which confirms that pulsation will not change the shape of ZOIs and the size of ROIs. However, no microscopic observation was made to confirm whether the air bubbles and channels change shape or move with ZOIs. Hence, the effectiveness of pulsation to improve the efficiency of air sparging cannot be evaluated using the repeatability evaluation tests of this paper.

Table 3. Experimental Sets.

Group No.	Configuration No.	Initial Air-Injection Pressure (kPa)	Observation Purpose	Number of Experiments
1	C1	14, 40, 45, 57, 60,65	Effect of initial air-injection pressure on airflow pattern & Effect of further increase in air-injection pressure on airflow pattern.	5 × 3 = 15
2	C2	14, 40, 45, 57, 60,65		5 × 3 = 15

There were two different groups of experiments performed. The first group is referred to as Group A. This group is performed to study the effect of the air-injection pressure level on the initiation of air channels (creating new channels). The second group, referred to as Group B, is performed to study the effect of the increase in the air-injection pressure on already formed air channels (deforming old channels). Group A and B experiments were performed for both Configurations C1 and C2. Results of these two groups of experiments are compared to evaluate the effect of the thickness of the partially saturated zone (top dry or partially saturated layer) on the size of the ZOI. Each experiment was performed three times resulting in fifteen total tests for each configuration.

Group-A Experiments

All glass-bead configurations were prepared using the dry- and wet-pluviation methods described in the previous section. Then air was injected into the bottom of the saturated medium. Thereafter, the size of the projection of the zone of influence (ZOI) observed on the front side of the box for Configurations C1 and C2 was measured. The top views of the ZOI for Configurations C1 and C2 were not visible because of the existence of the partially saturated top layer. At the moment of air injection into the saturated medium (initial air injection), the ZOI was created, and the size of the ROI was established and remained constant over the time. After forming the ZOI, the size of the ROI was measured. Later on, the air-injection system was turned off. There are two options to achieve fresh systems: one is to empty the box and create a new sample using the dry- and wet-pluviation methods; the second option, which saves time, is to drain and recharge the water through the bottom of the box. The process of drainage-recharge includes draining the water through the bottom of the box, leaving the sample untouched for 24 hours (referred to as resting time) until air channels disappeared, and then re-saturating the glass-bead medium through the bottom with the exact amount of water as the first round (referred to as recharge). Draining water through the bottom, having a one-day resting time, and saturating the medium through the bottom provide a condition for the channels to disappear and prepare the sample for the next rounds.

It was necessary to prove that the two options create equally fresh samples and that the previous air injection has no effect on the drained-recharged samples. Hence, air injection was performed on both newly pluviated samples (referred to as virgin) and drained-recharged samples. The results of the ZOI measurement for virgin samples were the same as the ZOI measurement of drained-recharged samples. Therefore, the drainage-recharge procedure is sufficient to create fresh samples for measuring the ZOIs, which give the same results as those of the virgin samples. In other words, the drainage-recharge process helps eliminate all channels and prepare a sample exactly the same as freshly pluviated samples.

After drainage-recharge of the sample, the air-injection system was turned on to inject air at different initial pressure levels, and the projection of the ZOI was measured on the front of the box for Configurations C1 and C2. The ROI was measured and compared with the size of the ROI at different initial air-injection pressures for each configuration. The results for Configurations C1 and C2 are also compared to evaluate the effect of the thickness of the partially saturated top layer on the size and shape of the ZOI.

Group B Experiments

As mentioned for Group A, Configurations C1 and C2 were first prepared using the dry- and wet-pluviation method. Air was then injected into the bottom of the water-saturated medium at specific initial pressure levels for each configuration, and the size of the ROI was recorded. Then the air-injection pressure was further increased (without shutting down the air-injection system) to evaluate the effect of a further increase in air-injection pressure on the size of already formed ZOI. Thereafter, the samples were drained-recharged using the same method described for Group A, and the experiments were performed at other initial air-injection pressures followed by a further increase in the air-injection pressure to evaluate the effect of a further increase in air-injection pressure on the size of the ROI for various initial air-injection pressures.

Summary of Results

These two groups (Groups A and B) of experiments featured 0.8mm glass beads as a simulant for granular soil media. The glass-bead media include saturated and unsaturated zones prepared using wet- and dry-pluviation methods, subjected to hydrostatic water (no flow). Wet- and dry-pluviation methods provide very homogenous, saturated and unsaturated zones. These groups of experiments were performed to study the effect of initial air-injection pressure and a further increase in air-injection pressure on the size and shape of the ZOI. As mentioned, air injection into the medium is initiated using various air-pressure levels from 14 to 60 kPa (the air-injection pressure measured at the entrance of the injection well). Thereafter, the airflow pattern was observed on the front face of the box. The airflow rate was measured using a flowmeter. Table 4 shows measured flow-rate values at different air-injection pressure levels.

Table 4. Airflow rate at different air-injection pressure levels.

Air-injection pressure (kPa)	Airflow rate (SCFH)
14	30
40	50
45	55
57	60
60	70

When air was injected at a pressure of 14 kPa into C1, the air formed channels, and the ZOI was cone-shaped (Fig. 7). The pressure was then further increased, and the airflow pattern was again observed to evaluate the effect of the further increase in the air-injection pressure on the size and shape of the ZOI. Even when the pressure was further increased to 60 kPa, the size and shape of the ZOI did not change.

Fig. 7. The side view of the ZOI for Configuration C1.

The maximum radius of influence (ROI) was reached right after the initiation of air injection and was not altered by any level of further increase in the air pressure. The experiment was repeated at different initial air-injection pressure levels to evaluate the effect of the initial air-injection pressure and further increase in air pressure on the size and shape of the ZOI. The results show that when the initial air-injection pressure is higher, the ROI will be larger, as shown in Fig. 8; however, no ROI change is observed with any further increase in the air pressure after the initial formation of the ZOI. For example, the ROI generated by the initial air-injection pressure of 45 kPa was measured to be 14.5 cm for C1, which never changed with the further increase in air pressure up to 60 kPa after the initial formation of air channels.

The radius of influence (ROI) was measured to be 16 cm at the initial air-injection pressure of 57 kPa and remained at 16 cm. On the other hand, 57 kPa seemed be a limit for the effect of the initial air-injection pressure. In other words, even initial air-pressure levels set beyond 57 kPa initiate an ROI limited at 16 cm. This limit seemed to be controlled by the overburden glass-bead pressure. Based on these results, a limit in the size of the radius of influence (ROI) has been reached when the initial air-injection pressure was set at 57 kPa for C1. This limit in value is expected to depend on the overburden pressure (i.e., the effective vertical stress due to the glass beads above), box geometry, and the grain-size distribution of the porous medium. Effective stress is the equivalent distributed (over the gross area) stress due the contact pressure between soil grains. Effective stress can be calculated by subtracting the pore-water pressure from the total stress.

These groups of experiments (Groups A and B) were also performed for Configuration C2 and at the same condition (airflow rate, air-injection pressure). As shown in Table 2, Configuration C2 has a different thickness of partially saturated zone from Configuration C1. The airflow pattern was then observed on the front face of the box, as in Configuration C1. The results show that air moved in channels, and the shape of the ZOI was cone-shaped, but the size of the ROI increased in comparison with the ROI in Configuration C1 at the same initial air-injection pressure. The effect of overburden (i.e., the difference in the thickness of the partially saturated zone) on the size of the ZOI can be studied by comparing the results of Configurations C1 and C2. The results also illustrate that, similarly, the size of the ROI did not increase in spite of any further increase in the air-injection pressure for C2 either. The experiment was performed at various initial air-injection pressure levels and then the pressure was further increased. The effect of a further increase in air-injection pressure for both C1 and C2 are shown in Fig. 9.

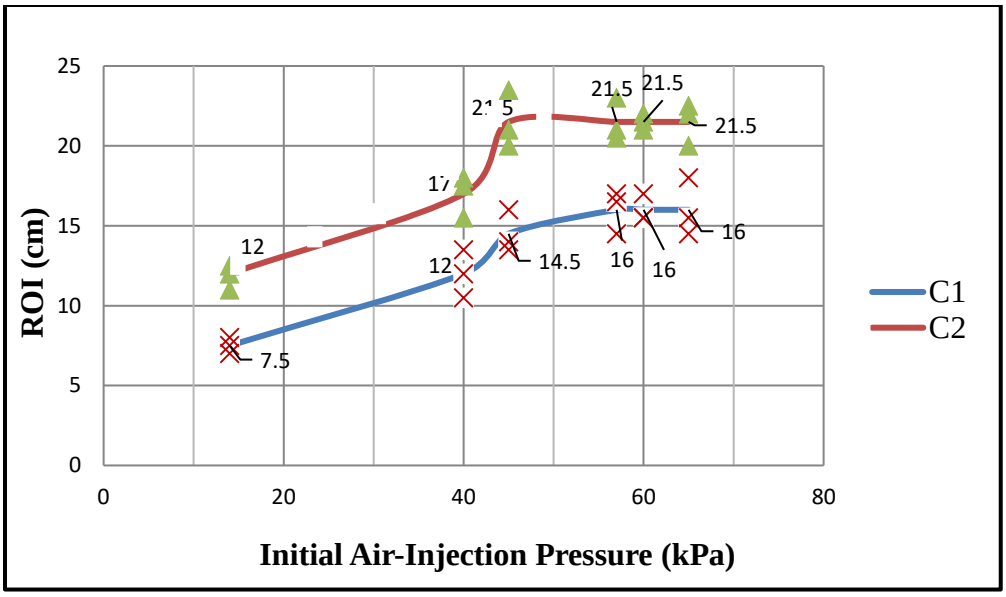

Fig. 8. The effect of an increase in the initial air-injection pressure (Group A), Configurations C1 and C2. Three trials were performed, whose results are shown.

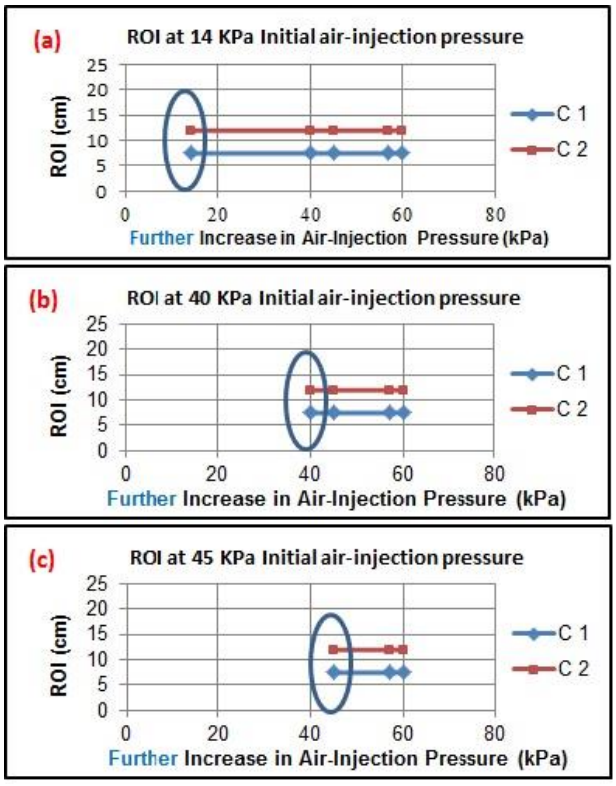

Fig. 9. The effect of a further increase in air-injection pressure (Group B), Configurations C1 and C2 at various initial air-injection pressures: a) 14 kPa, b) 40 kPa, and c) 45 kPa.

To summarize, the results show that the increase in the initial air-injection pressure results in a larger ROI; however, a further increase in the air pressure after air channels are already formed may affect the air concentration within the air channels but has no effect on the ROI. The radius of influence increased from 12 cm to 21.5 cm when the initial air-

injection pressure increased from 14 kPa to 45 kPa for Configuration C2 (Fig. 9). For the geometry of the box, the ROI remained constant at 21.5 cm when the initial air pressure was increased further up to 57 kPa. Air-injection pressures higher than 57 kPa can disturb the glass-bead packing and move the glass-bead grains. Hence, there is a limitation for each configuration based on the thickness of the partially saturated zone (effective overburden pressure). Based on these results, the same limit on the size of the ROI has been reached in smaller initial air-injection pressures for Configuration C2 compared to Configuration C1. The ROI size as a function of the initial air-injection pressure is shown for Configurations C1 and C2 in Fig. 9. In other words, this limiting value of ROI for the initial air-injection pressure still exits for the porous medium and box geometry based on the overburden pressure. However, it is reached at a lower air-pressure level.

The results show that the ROI of the formed channels is decided by the initial air-injection pressure. Fig. 9 shows that at a constant pressure, the size of the ROI will increase by increasing the overburden thickness of the partially saturated zone. By increasing the thickness of the partially saturated zone, the effective vertical stress at the level of the bottom of the air-injection well increases; then the ZOI at a higher overburden can be larger, even at the same initial air-injection pressure (Fig. 10). In other words, the size of the ROI is decided by the magnitude of the initial air-injection pressure and the overburden pressure (in this case, controlled by the contrasting thickness of the partially saturated zone). The ROI is, hence, a function of the initial air-injection pressure and overburden pressure. The results also show that the ROI of the formed channels, decided by the initial air-injection pressure, does not change by any further increase in air pressure. In other words, the resulting fully formed channels are very stable and will not change by any further increase in air-injection pressure. Within the unstimulated test (Group A), no further increase in air-injection pressure can change the ZOI shape and ROI size of already formed channels.

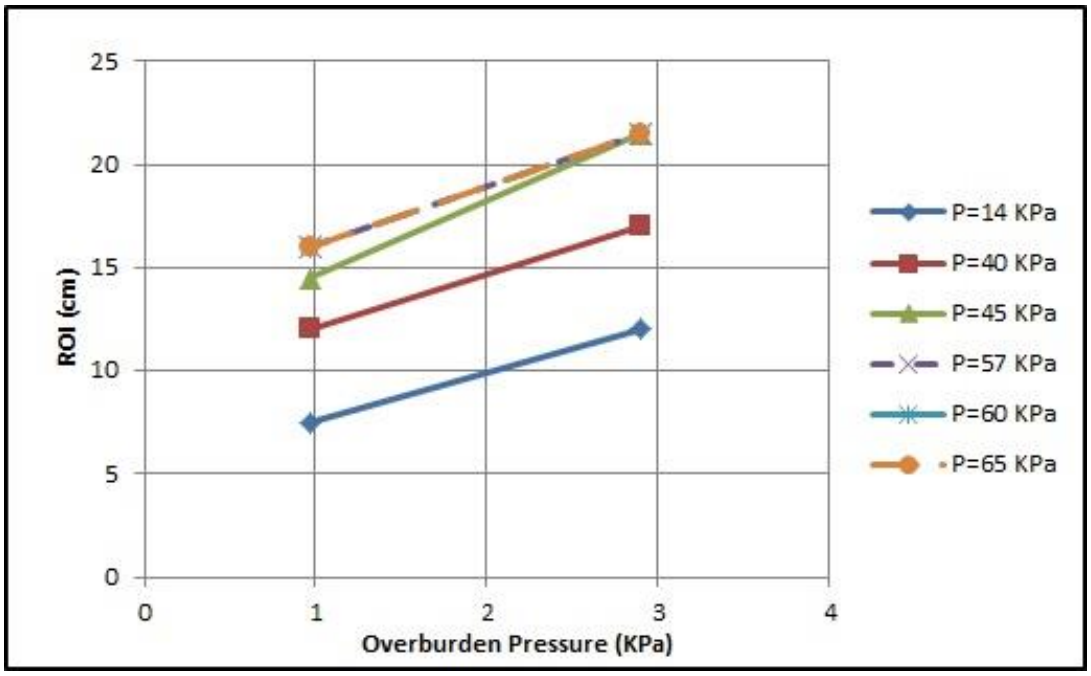

Fig. 10. The effect of overburden pressure in different air-injection pressures on the ROI.

Conclusions

This research investigates the effect of air pressure levels on air-channel formation during air sparging. This study investigated the effect of the overburden pressure at the injection depth (through variations in the partially saturated thickness of the porous medium) on characteristics of an unstimulated (i.e., no EM waves) ZOI during air sparging. On the other hand, the results of this paper are needed to study the effects of electromagnetic waves (EM) stimulation on the ZOI in another companion paper (Farid et al., 2017). To reach the goal, two experimental configurations (C1 and C2) with different overburdens (by various thicknesses of partially saturated zones) were designed. Then the effects of the initial air-injection pressure on initiation of the ZOI and the effect of a further increase in the air-injection pressure on the already formed ZOI were studied.

The results show that the side view of the shape of the ZOI is cone shaped for Configurations C1 and C2. The overburden (in this case, varied by varying the thickness of the partially saturated layer of glass beads) plays a role in determining the size of the ZOI (i.e., ROI) during air sparging. At equal initial air-injection pressure, the configuration with a higher overburden pressure (due to a thicker partially saturated zone of glass beads) has a larger ROI in comparison with the configuration with a lower overburden pressure (due to a thinner partially saturated zone). The initial air-injection pressure is also another determinative factor on the size of the ZOI (i.e., ROI). Larger initial air-injection pressure levels lead to a larger size of the ZOI (i.e., ROI) for all configurations.

In other words, there is a limitation for the ROI, regardless of how high the initial air-injection pressure reaches, for any specific geometry and overburden pressure. This limitation of ROI is different for each configuration with different overburden pressures (due to various thicknesses of the partially saturated glass-bead layer). The configuration with a higher overburden pressure (i.e., a thicker partially saturated zone of glass beads) reaches the limitation of the ROI at a lower air-injection pressure in comparison with the configuration with a lower overburden pressure (due to a thinner partially saturated zone).

However, a further increase in air-injection pressure has no effect on the shape and size of the ZOI. In other words, already formed ZOIs are very stable and hard to alter. After formation of air channels, the shape and size of the ZOI does not change even under large further increases in air-injection pressure. This work and its results are referred to as an unstimulated study since a similar study has been performed to investigate the effects of EM waves on the airflow pattern during air sparging, which is presented in a companion paper (Farid et al., 2017).

Acknowledgements

This research was supported by National Science Foundation through the Interdisciplinary Research (IDR) program, CBET Award No. 0928703. The authors also thank Vahab Bolvardi and Ruth Paul for their help with the preparation of the paper.

List of Notation

AS	Air Sparging
EM	Electromagnetic Wave
MTZ	Mass Transfer Zone
ROI	Radius of Influence
SVE	Soil Vapor Extraction
VOC	Volatile Organic Compound
ZOI	Zone of Influence

References

Azad, M., Sangrey, H. D. O., Farid, A., Browning, J., and Barney Smith, E. (2013). "Electromagnetic stimulation of two-phase transport in water for geoenvironmental applications." *ASTM, Geotechnical Testing Journal*, 36(1), 97-106.

Bayat, E. E., Yegian, M. K., Alshawabkeh, A., and Geokyer, S. (2009). "A new mitigation technique for preventing liquefaction-induced building damages during earthquakes*." WCCE – ECCE – TCCE Joint Conference: Earthquake & Tsunami*.

Benner, M. L., Mohtar, R. H., and Lee, L. S. (2002). "Factors affecting air sparging remediation systems using field data and numerical simulations." *Journal of Hazardous Materials*, B95, 305–329.

Braida, W., and Ong, S. K. (2001). "Air sparging effectiveness: Laboratory characterization of air channel mass-transfer zone for VOC volatilization." *Journal of Hazardous Materials*, B87, 241-258.

Brooks, M. C., Wise, W. R., and Annable, M. D. (1999). "Fundamental changes in in-situ air sparging flow patterns." *National Ground Water Association*, 105-113.

Elder, C. R., and Benson, C. H. (1999). "Air-channel formation, size, spacing, and tortuosity during air sparging." *National Groundwater Association*, GWMR, 171-181.

Farid, A., Azad, M., Browning, J., and Barney-Smith, E. (2014) "Electromagnetically induced transport in water for soil/groundwater remediation," *ASCE Journal of Geoenvironmental & Geotechnical Engineering*, 141(3), 04014115-1 – 0404115-10, March, DOI: http://dx.doi.org/10.1061/(ASCE)GT.1943-5606.0001244.

Farid, A., Najafi, A., Browning, J., and Barney-Smith, E. (2017). "Air sparging 2: Electromagnetic waves' effect on airflow pattern." *ASCE, Journal of Geotechnical and Geoenvironmental Engineering*, Simultaneously Under Review.

Hu L., Wu, X., Meegoda, J. N., and Gado, S. (2010). "Physical modelling of airflow during air sparging remediation." *Environmental Science Technology*, 44(10), 3883-3888.

Ji, W., Dahmani, A., Ahlfeld, D. P., Lin, J. D., and Hill III, E. (1993). "Laboratory study of air sparging: Airflow visualization." *Groundwater Monitoring and Remediation*, 115-126.

Johnson, R. L., Johnson, P. C., McWhorter, D. B., Hinchee, R. E., and Goodman, I. (1998). "An overview of in-situ air sparging." *Journal of Groundwater Monitoring and Remediation*, 13(4), 127-135.

Lundegard, P. D., and Anderson, G. (1996). "Multiphase numerical simulation of air sparging performance." *Groundwater*, 34(3), 451-460.

Marley, M. C., Droste, E. X., and Bruel, C. J. (1996). "Use air sparging and vapor extraction to remediate subsurface organics. Wastewater and groundwater Treatment." <Last accessed in February 2017, http://www.globalspec.com/reference/9391/349867/use-air-sparging-and-vapor-extraction-to-remediate-subsurface-organics>

Michael, J., and Ken, B. (2006). *Soil liquefaction: A critical-state approach*, CRC Press. ISBN 020330196X, 9780203301968, <Last accessed in February 2017, http://books.google.com/books?id=E9shjoVdEl0C&pg=PA421&lpg=PA421&dq=wet+pluviation+method+ishihara&source=bl&ots=qfjM4wpQ0Y&sig=S6eVtzlgKdb0Tpa8whvKHXARhH4&hl=en&sa=X&ei=tUN-U9OFJdefyASJ0ILIDg&ved=0CDAQ6AEwAQ#v=onepage&q=wet%20pluviation%20method%20ishihara&f=false>

Nyer, E. K., and Suthersan, S. S. (1993). "Air sparging savior of groundwater remediation or just blowing bubbles in the bathtub." *Groundwater Monitoring Review*, 13(4), 87-91.

Reddy, K. R., Kosgi, S., and Zhou, J. (1995). "A review of in-situ air sparging for the remediation of VOC-contaminated saturated soils and groundwater." *Hazardous Waste and Hazardous Materials Journal*, 12(2), 97-118.

Reddy, K. R., and Adams, J. A. (2001). "Effect of soil heterogeneity on airflow patterns and hydrocarbon removal during in-situ air sparging." *ASCE Journal of Geotechnical and Geoenvironmental Engineering*, 127(3), 234-247.

Semer, R., Adams, J. A., and Reddy, K. R. (1998). "An experimental investigation of airflow patterns in saturated soils during air sparging." *Geotechnical and Geological Engineering*, 59-75.

Semer, R. (1998). *Air sparging: Contaminant removal mechanisms parameterization comparisons, and enhancement*, MS Thesis, University of Illinois at Chicago.

Suthersan, S. S., and Raton, B. (1999). "In-situ air sparging, remediation engineering, design concepts." *CRC Press LLC*, <Last accessed in February 2017, http://www2.bren.ucsb.edu/~keller/courses/esm223/SuthersanCh04AirSparge.pdf>

Vaid, Y. P., and Negussey, D. (1998). "Preparation of reconstituted sand specimens: Advanced triaxial testing of soil and rock." *ASTM*, STP 977, Philadelphia, 405-417.